Turk J Phys
29 (2005) , 371 – 378.

Origins of Reverse Bias Currents in a Typical BPW34 Photodiode

Habibe BAYHAN, Şadan ÖZDEN
University of Muğla, Faculty of Art and Science, Department of Physics
48000 Muğla-TURKEY
e-mail: hbayhan@mu.edu.tr

Received 14.09.2005

Abstract

Measurements of the dark reverse current in a typical BPW34 silicon photodiode have been made in the temperature range 100–300 K at various reverse bias voltages ranging from 0 to 60 V. Various transport models have been applied to analyze the temperature dependence of the reverse current-voltage data. We suggest that Bardeen's model for a modified Schottky-like interfacial junction, that takes into account the effect of interfacial localized states, can be satisfactorily applied to describe the reverse current-voltage characteristics at bias voltages below 50 V.

Key Words: BPW34, PIN, Photodiode, reverse bias, current transport.

1. Introduction

The silicon BPW34 PIN photodiode is widely used in many applications such as photo-interrupters, IR sensors, industrial electronics, and control and drive circuits. In any type of junction structure, PN or PIN, leakage (dark) reverse current is detrimental to device performance. The value of leakage current could be extremely small to allow a very large dynamic range to the device. To optimize the device performance of BPW34-like photodiodes, it is essential to understand the electrical conduction mechanisms for the dark reverse-bias leakage current. The possible origin of this leakage current in silicon PN and PIN devices is commonly described by a combination of diffusion and generation components [1–6]. The diffusion current is caused by the minority carriers generated in the neutral regions and diffused to the edge of space charge region. The generation phenomena is thermally activated and field assisted, and seems to be related to processing technology and the fundamental properties of silicon.

The present investigation describes the dark reverse bias electronic transport properties of a typical BPW34 (Vishay) photodiode by temperature dependent current-voltage (I-V-T) measurements. The primary purpose of this paper is to elucidate the behaviour of the experimentally observed reverse I-V-T characteristics of this PIN photodiode using the existing electrical conduction models to determine the predominant charge transport mechanism(s) operable in this device. We propose that Bardeen's model for a modified Schottky-like interfacial junction successfully explains the reverse current-voltage characteristics of a typical BPW34 photodiode at the temperature range studied.

2. Experimental

The standard current-voltage (I-V) measurements of BPW34 (Vishay) photodiodes were carried out in the dark and in an experimental set-up consisting of closed-cycle helium cryostat (Oxford), a programmable temperature controller (ITC 502) and a source-measure unit (Keithley 236). The device was mounted in the sampler holder of the cryostat and the measurements were made in vacuum at temperatures between 100 and 300 K in steps of 20 K.

3. Results and Discussions

Figure 1 shows a typical set of experimental dc reverse-bias current-voltage curves of a typical BPW34 photodiode in the voltage range between 0–60 V at different ambient temperatures. The figure reveals the existence of three distinct regions of IV curves. A relatively strong bias dependence of the reverse current observed in region I could be due to the recharging of trapping states within the junction region [7]. Reverse current shows a weak dependence both on the temperature and the voltage in region III. It is natural to suggest that this almost unchanged behaviour at relatively high reverse biases (>50 V) is due to strong electric field effects [2].

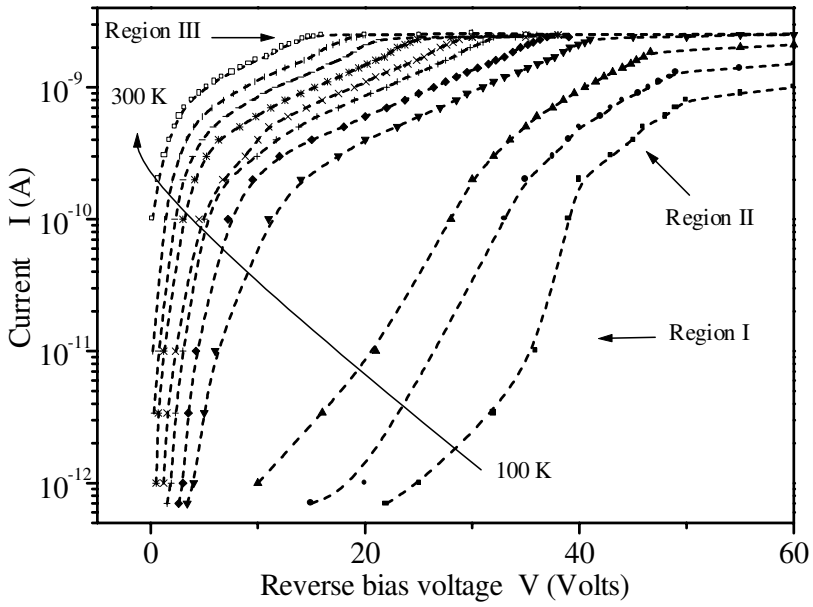

Figure 1. The dark reverse IV characteristics of a typical BPW34 (Vishay) photodiode at various temperatures. The dotted lines are present to guide the eye.

In order to identify the dominant current transport mechanism in region II, the reverse I-V-T curves were examined using various conduction models. Figures 2 and 3 suggest that the reverse conduction is dominated neither by space-charge limited current (SCLC) nor the generation mechanism [8].

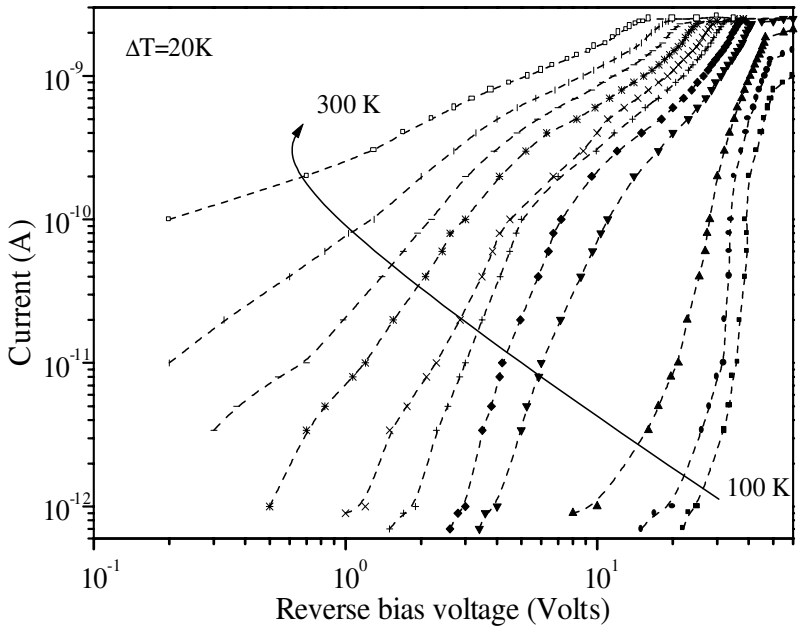

Figure 2. The Log I – Log V characteristics of a typical BPW 34 (Vishay) photodiode at various temperatures. The dotted lines are present to guide the eye.

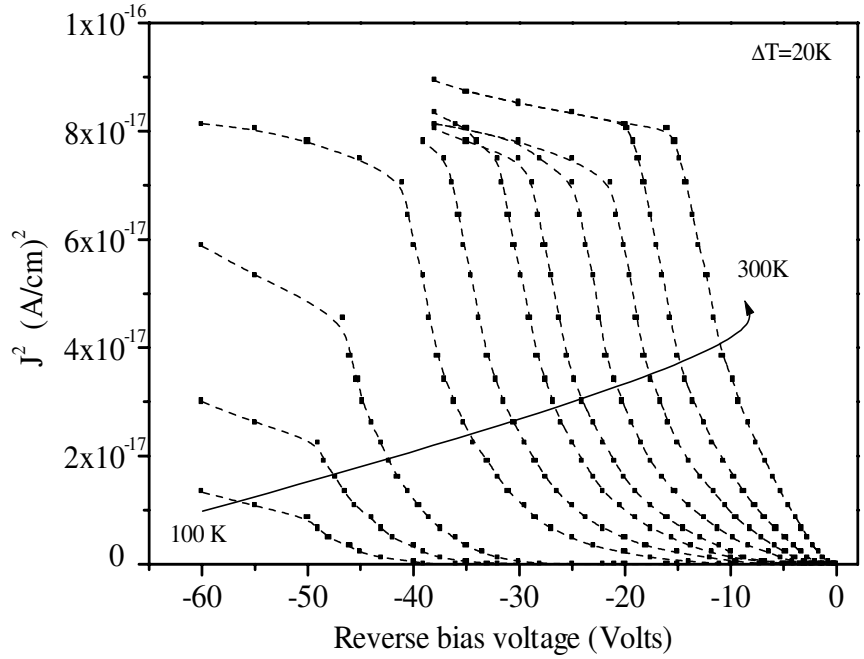

Figure 3. Square of current density vs. reverse bias voltage. The dotted lines are present to guide the eye.

Figure 4 shows the temperature dependence of the reverse current of a typical photodiode, plotted as $\mathrm{Log}(I_R)$ as function of $1000/T$ at different reverse-bias voltages between 0.5 and 25 V. As the Arrhenius plots appear to exhibit a thermally activated behavior, we expect the reverse current can be expressed as [9]

$$I_R(T) \propto \exp\left(-E_a/kT\right), \tag{1}$$

where E_a is the activation energy and k is the Boltzmann constant. The inset in Figure 4 shows E_a as a function of $\sqrt{V}$, V being the bias voltage; note the quality of the linear trends. A possible physical origin for the observed variation of E_a could be related to localized defect states in the band gap of the depletion (intrinsic) layer [9, 10]. Therefore, the reverse current may possibly be controlled by currents due to Poole-Frenkel and Schottky mechanisms [10].

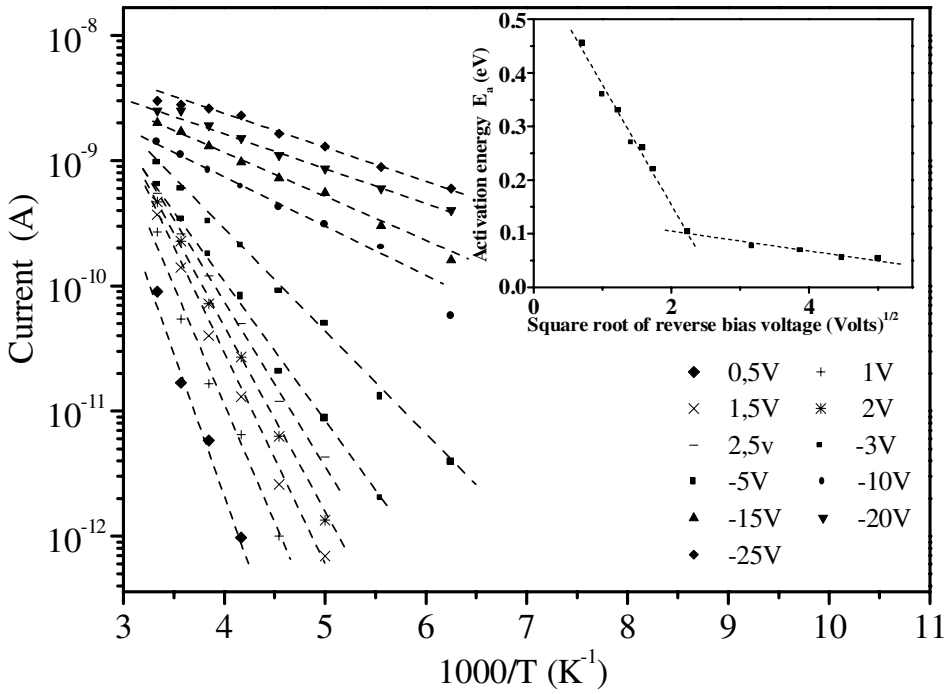

Figure 4. The semi-Log I vs. $1000/T$ characteristics at various reverse voltages. The inset shows the reverse bias-voltage dependence of the activation energy E_a. The dotted lines correspond to best linear fits.

The current-voltage characteristics for the Richardson-Schottky/(classical) Poole-Frenkel effect can be expressed [8, 11–17] via the equations

$$I(V,T) = BV^{\gamma} \exp\left[-\frac{e\Phi(V)}{kT}\right] \tag{2}$$

$$\Phi\ (V) = \Phi_o - n\left(\frac{e\eta}{4\ \pi\varepsilon_o\,\varepsilon_r\,\chi\,d}\right)^{1/2} V^{\,1/2}, \tag{3}$$

where $e\Phi\ (V)$ is a voltage dependent activation energy which represents a Schottky-barrier height or defect energy; $e\Phi_o$ is its zero voltage value; e is the electronic charge; ε_o is the permittivity of free space; ε_r is the optical dielectric constant of the material; and B is a parameter which depend on material properties, applied voltage and temperature.

For a modified Poole-Frenkel mechanism [14, 15] $\gamma = 1$, $n = 2$, $\eta = 2$ and $e\Phi_o = E_o = 0$ (zero field, i.e. trapping/ionizable center energy [13]), and $\chi\,d(=\omega)$ is the width of the interfacial depletion region (the

parameter χ accounts for the uniformity in the distribution of electric field at junction interface). The $V^{1/2}$ prefactor defined in the Φ (V) relation in equations (2) and (3) are often written singly in terms of the Poole-Frenkel coefficient $\beta_{PF} = (e/\pi\,\varepsilon_o\,\varepsilon_r)^{1/2}$.

For the Schottky mechanism, $n = \eta = 1$, $\gamma = 0$ and $B = SA^{**}T^2$, where S is the effective contact area and A^{**} is the effective Richardson constant. The corresponding I-V relation according to the Simmons's model is given by the Richardson-Schottky formula [14]

$$I_s(V,T) = I_{so}\ \exp\left[\frac{e\,\beta_s\,V^{1/2}}{k\,T\,\omega^{1/2}}\right] \tag{4}$$

$$I_{so} = S\,A^{**}\,T^2\ \exp\left[-e\Phi_o/kT\right], \tag{5}$$

where $\beta_s = \beta_{PF}/2$ is the Schottky coefficient.

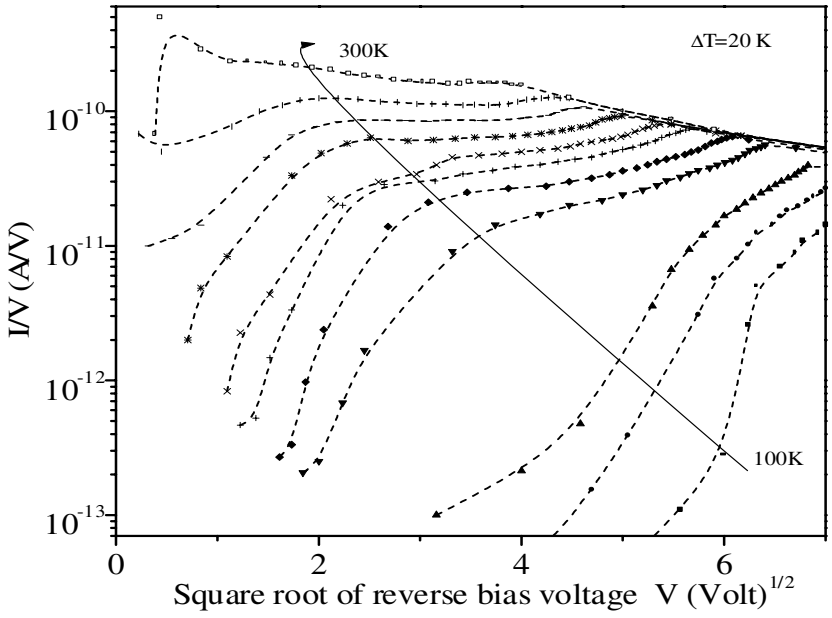

Figure 5. Log I/V vs. $V^{1/2}$ characteristics in the temperature range between 100 and 300 K. The dotted lines are present to guide the eye.

The experimental data was analyzed by plotting Log(I/V) against $V^{1/2}$ (see Figure 5) and Log I against $V^{1/2}$ (see Figure 6) to explore the presence of Poole-Frenkel and Schottky-type mechanisms, respectively. Figures 5 and 6 reveal that the Log I vs. $V^{1/2}$ plot give visually good linear regions which are denoted as 1 and 2 as compared to variations in the Log(I/V) vs. $V^{1/2}$ plot. This suggests that Schottky-type conduction can be a dominant mechanism. Thus equations (4) and (5) can be applied to describe the temperature and bias dependence of the reverse bias current. Both the pre-exponential current factor $I_{so}(T)$ and m_s values were determined from the intercept of linear variations on the current axis and from the slope of the linear regions (1 and 2), respectively. The temperature dependence of $I_{so}(T)$ and m_s are plotted as $\ln I_{so}\,T^{-2}$ vs. $1/T$ and m_s vs. $1/T$ and are shown in Figure 7. From the slopes of the linear variations in ln $I_{so}\,T^{-2}$-$1/T$ plot, the zero field Schottky-like barrier height values were calculated as about 0.40 eV and 0.10 eV for regions 1 and 2, respectively.

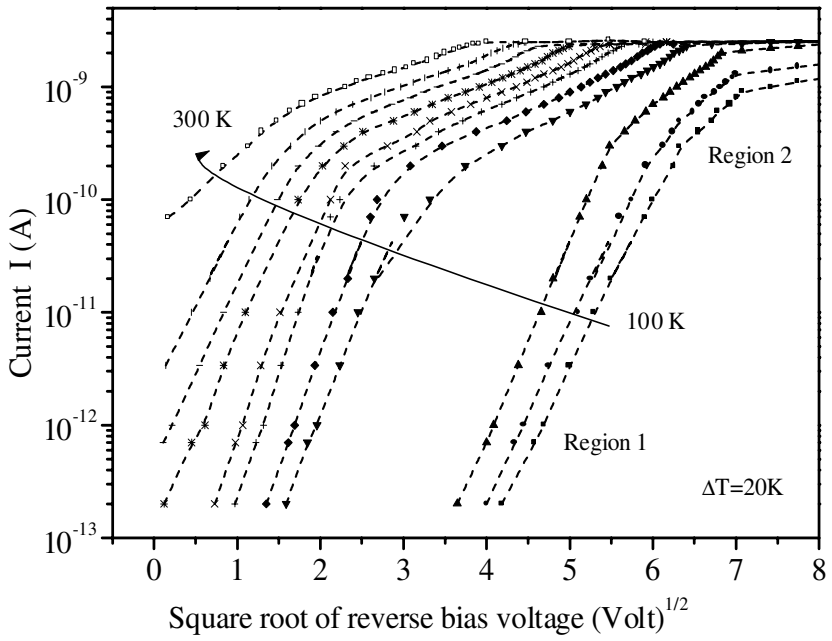

Figure 6. Log I vs. $V^{1/2}$ characteristics in the temperature range between 100 and 300 K. The dotted lines are present to guide the eye.

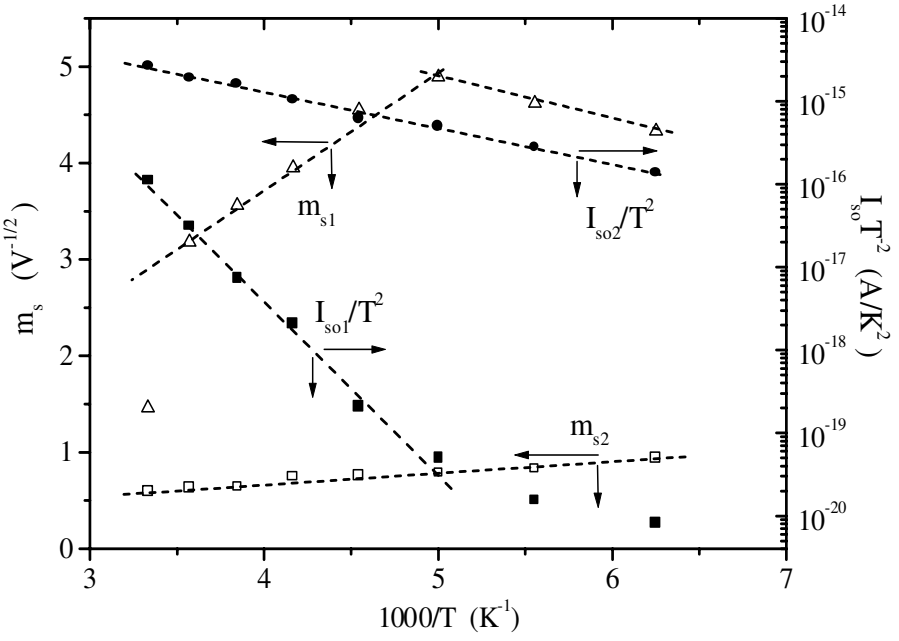

Figure 7. The temperature dependence of pre-exponential current factor $I_{so}(T)$ and the slope m_s of the Richardson-Schottky formula in regions 1 and 2 of Figure 6. The dotted lines correspond to best linear fits.

Plots of m_s as a function of $1000/T$ (Figure 7) are used to calculate Schottky coefficients. The values of m_s are found to be scattered about a value of 0.8 $V^{-1/2}$ in region 2. However in region 1, a linear trend is

obtained for a limited temperature range (220–280 K) and less temperature dependent behavior is observed below 220 K. Using the values of $m_{s_{1,2}}$ evaluated at 220 K, and $\omega = 0.07$ cm for the width of the depletion region, the experimental values of Schottky coefficients $\beta_{s,\mathrm{exp}} \sim 0.23{\times}10^{-3}$ $\mathrm{V}^{1/2}$ $\mathrm{m}^{1/2}$ and $0.04{\times}10^{-3}$ $\mathrm{V}^{1/2}$ $\mathrm{m}^{1/2}$ were estimated for regions 1 and 2, respectively, and are shown in Table 1. The theoretical value of the Schottky coefficient is calculated as about $1.1{\times}10^{-5}$ $\mathrm{V}^{1/2}$ $\mathrm{m}^{1/2}$ using $\varepsilon_r = 11.8$ for silicon. The difference between the theoretically calculated and experimentally deduced values of the Schottky coefficient may be intelligible if we assume that localized states which are proposed to be exist at or close to the p/i interface behave as the Schottky-like contact. Bardeen's model [16, 17] gives an expression for the junction current that includes the effect of interface states

$$I_{rev}(V,T) = I_{so} \exp\left(\frac{\beta_{sc}\, V^{1/2}}{kT}\right) \tag{6}$$

$$\beta_{sc} = \left(\frac{\delta\varepsilon_o\varepsilon_r}{\varepsilon_i + e\delta D_s}\right)\left(\frac{2e^3 N}{\varepsilon_o\,\varepsilon_r}\right)^{1/2}. \tag{7}$$

In this relation, β_{sc} is named as the modified Schottky constant. Theoretical value of β_{sc} was calculated using the interfacial region of thickness $\delta = 9$ μm, permittivity $\varepsilon_i = 3.8\,\varepsilon_o$, impurity concentration $N = 8.2{\times}10^{14}$ cm^{-3} and density of states $D_s \sim 10^{16}$ $\mathrm{eV}^{-1}\mathrm{cm}^{-2}$ in the depletion region as about 0.013 eV $\mathrm{V}^{-1/2}$. The values for δ, N and D_s were estimated from the results of temperature dependent capacitance-voltage and capacitance-frequency measurements done on the same photodiode [18].

Table. m_s, theoretical and experimental Schottky coefficient β_s and modified Schottky constant β_{sc} evaluated at 220 K for region 1 and 2 of Figure 7.

	$\frac{m_s}{V^{-1/2}}$	$\frac{\beta_{s,\mathrm{exp}}}{(V^{1/2}m^{1/2})}$	$\frac{\beta_{s,\mathrm{theo.}}}{(V^{1/2}m^{1/2})}$	$\frac{\beta_{sc,\mathrm{exp}}}{(eVV^{-1/2})}$	$\frac{\beta_{sc,\mathrm{theo.}}}{(eVV^{-1/2})}$
Region 1	4.55	$0.23{\times}10^{-3}$	$1.1{\times}10^{-3}$	0.090	0.013
Region 2	0.80	$0.04{\times}10^{-3}$	$1.1{\times}10^{-3}$	0.015	0.013

Experimental values of $\beta_{sc,\,\mathrm{exp}}$ were estimated by considering m_s $(=\beta_{sc,\,\mathrm{exp}}/kT)$ data at 220 K (being nearly constant with the applied temperature) and is plotted in Figure 7 as is found to be about 0.090 eV $\mathrm{V}^{-1/2}$ and 0.015 eV $\mathrm{V}^{-1/2}$ for regions 1 and 2, respectively. The reasonably good agreement between the theoretically and experimentally deduced values of modified Schottky constant β_{sc} suggests that the revere current-voltage-temperature behavior of the BPW34 photodiode may well be described by Bardeen's model for a modified Schottky-like interfacial junction. Since the i-region of BPW 34 is slightly n-type, and the mobility of electron is larger than that of holes, we expect that the p/i interface is likely to play a more relevant role for electrical conduction. Although we do not know the definite energy band structure of the PIN photodiode, we propose that the defect states possibly located at or close to the p/i interface behave as Schottky like barriers with activation energies 0.40 eV and 0.10 eV for regions 1 and 2 respectively.

4. Conclusion

The measured dark reverse bias current-voltage-temperature characteristics of a typical BPW34 photodiode have been examined using the currently existing transport models. We found that both space-charge limited current (SCLC) and generation mechanisms are not operable in the device. However, the temperature dependence of reverse bias current at different voltages (0.5–25 V) indicated the presence of thermally activated behavior in the device. The voltage dependence of the activation energy E_a of this behavior

through $V^{1/2}$ dependence was related to the presence of Poole-Frenkel or Schottky type conduction mechanisms. It was shown that Schottky type conduction seems to be highly operable and the possible origin of the reverse bias leakage current is proposed to be satisfactorily explained with Bardeen's model for a modified Schottky-like barrier probably due to energetic distribution of trap states at or close to the p/i interface.

References

[1] R. A. Street, *Appl. Phys. Lett.*, **57**, (1990), 1334.

[2] J. K. Arch and S.J. Fonash, *Appl. Phys. Lett.*, **60**, (1992), 757.

[3] F. Lemni, *J. Non-Crys. Solids.,* **266**, (2000), 1198.

[4] A. Ruzin and S. Marunko, *Nuc. Ins. And Meth. in Phys. Res. A.*, **494**, (2002), 411.

[5] S. Tchakarov, P. Roca i Cabarrocas, U. Dutta, P. Chatterjee and B. Equer, *J. Appl. Phys.*, **94**, (2003), 7317.

[6] A. Ruzin and S. Marunko and T. Tilchyn, *Nuc. Ins. And Meth. in Phys. Res. A.*, **512**, (2003), 21.

[7] Zs. J. Horváth, in S. K. Agarwal (Eds)., *Physics of Semiconductor Devices*, Narosa Publ. House, New Delhi, India, 1998.

[8] B. L. Sharma and R. K. Purohit, Semiconductor Heterojunctions, Oxford, Pergamon, 1974.

[9] A. Czerwinski, E. Simoen, A. Poyai and C. Claeys, *J. Appl. Phys.*, **94**, (2003), 1218.

[10] H. Chaabane, M. Zazoui, J. C. Bourgoin and V. Donchev, *Semicond. Sci. Technol.*, **8**, (1993), 2077.

[11] S. M. Sze, *Physics of Semiconductor Devices,* 2^{nd} ed., New York, Wiley, 1981.

[12] M. Shur, *Physics of Semiconductor Devices*, Englewood Cliffs, NJ, Prentice-Hall, 1990.

[13] M. M. Abdul-Gader Jafar, *Semicond. Sci. Technol.*, **18**, (2003), 7.

[14] J. R. Yeargan, H. L. Taylor, *J. Appl. Phys*,. **39**, (1968), 5600.

[15] X. Mathew, J.P. Enriquez, P.J. Sebastian, M. Pattabi, A. Sanchez-Juarez, J. Campos, J.C. McClure and V.P. Singh, *Solar Energy Mater. Sol. Cells.,* **63**, (2000), 355.

[16] E. H. Rhoderic, *Metal Semiconductor Contacts*, Oxford, Clarendon, 1978.

[17] A. E. Rakhshani, Y. Makdisi, X. Mathew and N.R. Mathews, *Phys. Status solidi a.*, **168**, (1998), 177.

[18] Ş. Ozden, *MS Thesis,* Muğla University, Muğla-TURKEY, 2005.